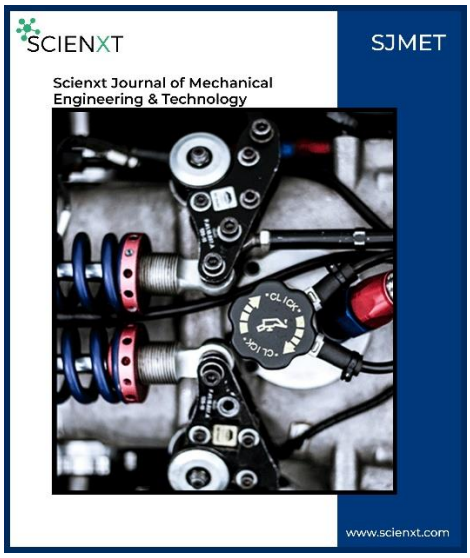

Scienxt Journal of Mechanical Engineering & Technology
Year-2023; Volume-1; Issue-1, pp. 13-26

Study of mechanical properties of pearlitic rail steel by modeling

Sonali Shinde[1], Parishwad Gaeakwad*[2], Shibanjan Paul Roy[3]

[1]Lecturer, Department of Mechanical Engineering,
K.J. Somaiya College of Engineering, Vidya Vihar Mumbai, Maharashtra, India
[2] Department of Mechanical Engineering,*
K.J. Somaiya College of Engineering, Vidya Vihar Mumbai, Maharashtra, India
E-mail: parish@somaiya.edu
[3]Independent Scientist, Jalpaiguri, West Bengal, India

https://zenodo.org/deposit/8054087

*Corresponding author: Parishwad Gaeakwad

Table of Contents

List of Figures

Abstract:

Since mass and product movement are increasingly dependent on trains, tracks must be stronger and last longer. Rail steel's mechanical characteristics, especially strength and hardness, must be increased. Pearlitic rail steel grade 900A offers good tensile and impact qualities. Steel tested had good dividend and tensile strengths but limited elongation. Using an RVE model, the impact of the bainitic phase on pearlitic rail steels was examined. The phases' ultimate shear curves were defined by chemical composition. Thus, the relationship between predicted elastic modulus and tensile strengths as a function of bainite phase fraction was determined. This model determines rail steel's microstructure.

Keywords:

Rail Steel, Microstructure, Accelerated Cooling, Cooling Curves, Microstructure, Mechanical Properties, Pearlitic Steel, RVE Model, Bainite.

1. Introduction:

Rail transit is a crucial aspect of every country's infrastructure because it's easy, safe, and eco-friendly. The popularity of steel railroads. Globally, faster, more capable trains can carry more (Kazum et al., 2013). Thus, the rails are repeatedly loaded, causing a more serious disaster due to wear and tear (LONG and KHANNA, 2007). The railways' mechanical quality must improve. Due to their high strength, mild ductility, and enhanced fatigue behavior, ferritic pearlitic steels dominate the rail industry (Masoudi Nejad and Liu, 2021). Christodoulou et al. examined 900A rail steel fatigue and fracture. Flat S-N curves are fatigue-resistant. It wasn't fragile, as a fatigue fracture demonstrated. Reduce pearlitic lamellar gap to strengthen rails (Eustis, 2013). Changing rail steel's microstructure from pearlite to bainite has attracted a lot of interest since fine microstructure steel is hard to create. Bainitic rail steel has outstanding mechanical characteristics and fracture toughness. Flake, wear, and weld-resistant barite rail steels. Mechanical performance depends on rail steel's microstructure. This study examined 900A rail steel microstructures (Kazum et al., 2013). An FE-based RVE model was used to examine pearlite and bainite rail steel. Phase fraction and mechanical qualities are also discussed.

1.1 Aim:

The fundamental objective of this research is to analyze the grades of pearlitic rail steel as well as to analyze its mechanical properties.

1.2. Objective:

- To impact examination, in line with the ASTM E23 average, was used to measure the toughness of the studied rail steel.
- To examine the influence of mass fraction of each phase on steel performance.
- To investigate the impact of bainite on rail steel's overall stress-strain response.

1.3. Research question:

1) What were the microstructure characteristics of the 900A grade of rail steel?
2) What are the machine-driven belongings of railing steel through just a pearlite microstructure affected by the amount of bainite present?
3) What are the machine-driven belongings of the rail brand's bainite phase fraction?

2. Literature Review:

2.1. Pearlitic rail steel:

Carbon is a major rail steel alloying component due to pearlite's microstructure. The form and space between cementite lamellae are also essential (Krauss, 1995). Finer Pearlite combines strength and hardness. Pearlite purification is needed for pearlitic rail metals. Pearlite consists of soft ferrite and hard cementite. Hard carbide and ferrite's elastic/plastic flow give it more durability. FIGURE 1: Pearlitic rail steel. Cementite and ferrite are minerals. Interlamellar spacing is 0.3 microns (Krauss, 1995).

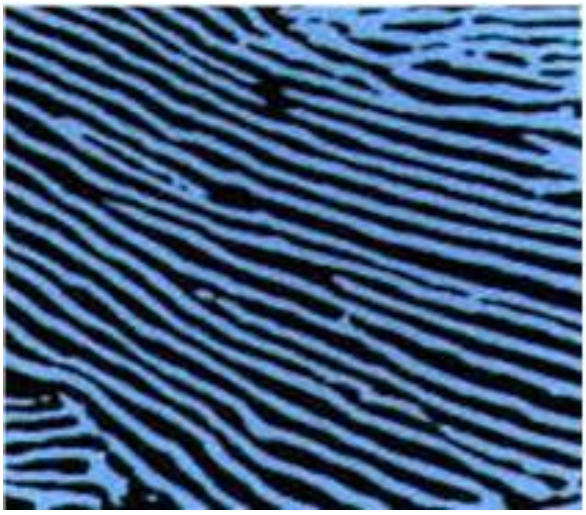

Figure.1: Microstructures of pearlitic rail steels [source: (Krauss, 1995)].

Pearlitic rail steel is commonly used in heavy-haul trains due to its lack of key alloying elements, low production costs, strong mechanical qualities, and wear resistance (Georgiev and Simeonova, 2019).

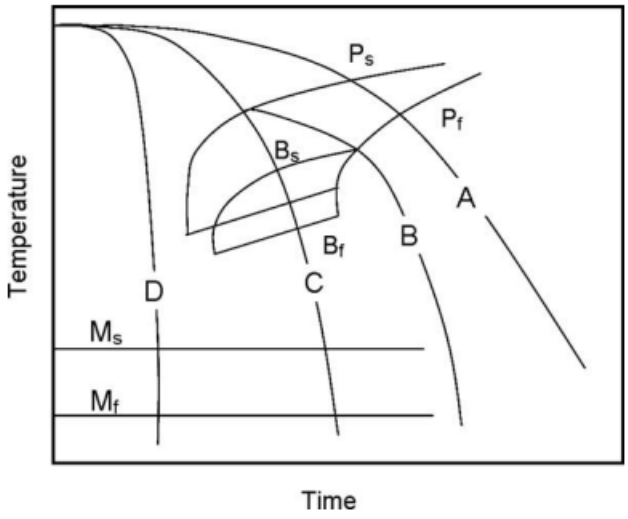

Figure.2: Outcome of chilling profile on the closing microstructure [source: (Olofsson et al., 2013)]

Abrasive, adhesive, erosion-percussion and fatigue wear reduce rail life. Train companies pay a lot each year to remove rolling contact fatigue cracks and spalls to improve service and prevent catastrophes. For track and wheels, pearlite, ferritic, and bainitic steels are employed. Microstructural railing steels through improved machine-driven and wears confrontation are addressed (Olofsson et al., 2013).

2.2. Quenching:

2.2.1. Heat transfer:

Quenching is key in steel thermomechanical processing. Amp vaporizable quenchant, such as by way of water, uses three fundamental thermal cooling methods for immersion quenching. When water first touches a heated metal, a vapor film forms, allowing full-film boiling FB to transfer heat to the water. Nuclear boiling NB happens when the temperature decreases toward the Leiden frost point, collapsing the vapor film and saturating the surface with liquid (Dean et al., 2009). Below the boiling point, convective cooling takes over and NB is no longer needed. Each of these cooling approaches is coupled to a specific heat transfer pathway (Fig. 3). (Hall and Mudawar, 1996). Given the many HTCs, this is crucial.

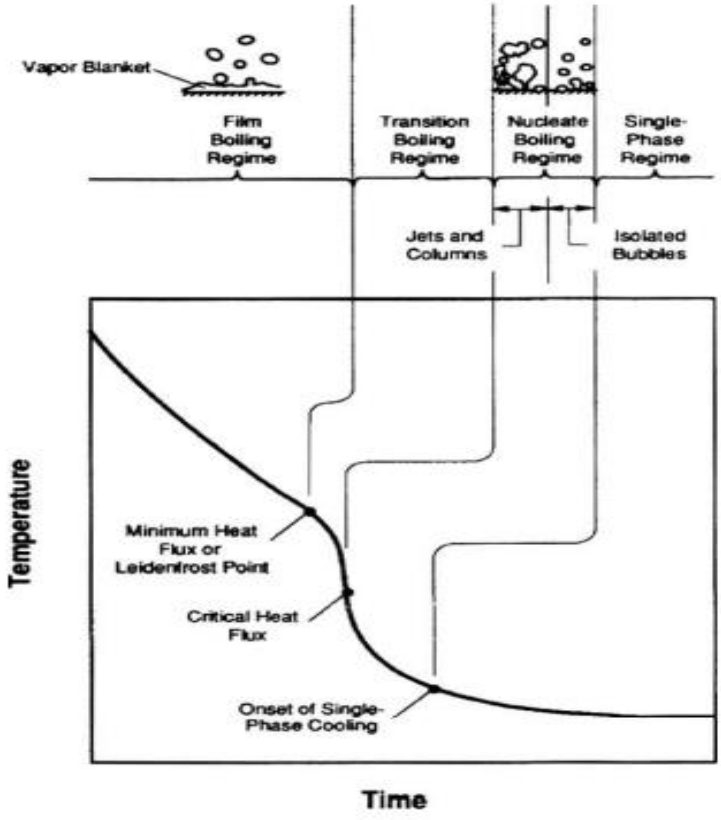

Figure.3: Diagram of cooling arc and the dissimilar cooling devices occurring from the time of initial absorption until the decision of the quench [source: (Hall and Mudawar, 1996)]

2.2.2. Quenchants:

As quenchants, a wide range of fluids have been employed, comprising air, rain, water, oil, and gases. The heat transfer rates of various quench media can be used to evaluate their effectiveness. If we compare the heat transfer rates of 3000–3500 w/m2 for circulating water with 50–80 w/m2 for still air, we notice that the latter has a far higher heat transfer rate. Figure 4 depicts the thermal efficiency of several gases. Experimentally measured chilling profiles are also used to calculate HTC, a measure of cooling media effectiveness. When utilizing finite element modelling, for example, the HTC is depicted in Fig. 5 (GRUSHKO et al., 2021).

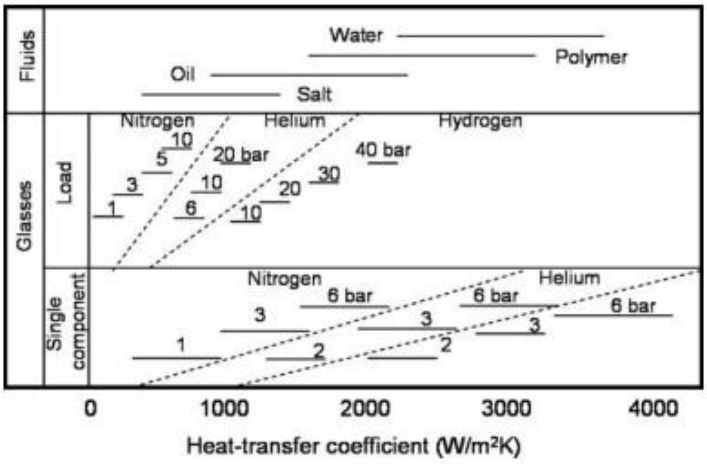

Figure.4: Assessment of HTCs realized with changedair quenching mass media [source: (GRUSHKO et al., 2021)]

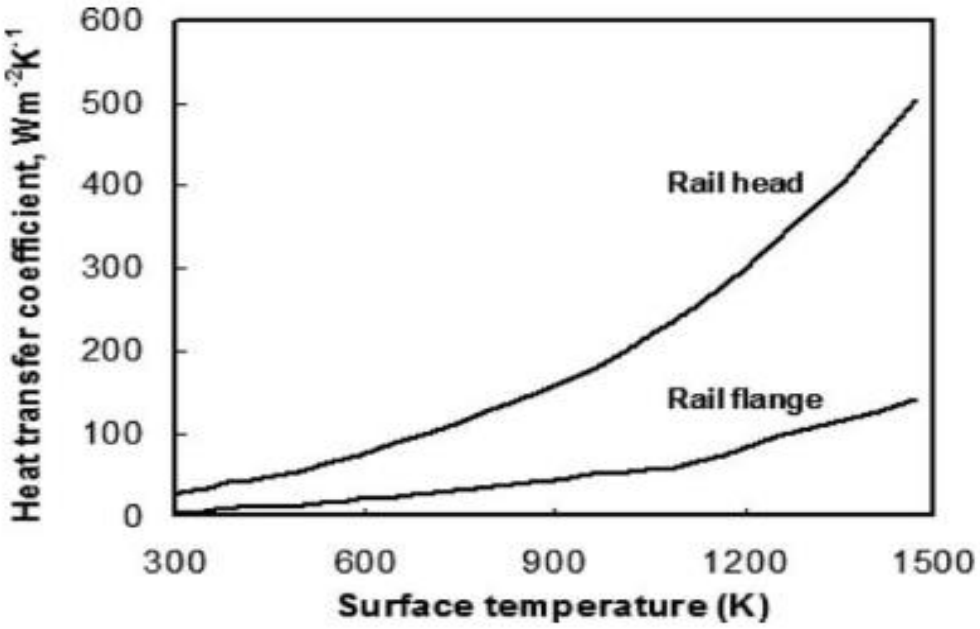

Figure.5: The HTC as a job surface fever for the head (dotted line) and projection (dashed line) found by using inverse analysis [source: (GRUSHKO et al., 2021)]

2.2.3. Spray quenching:

In Lenard 38, the result of outlet design, shape, then spray asset on rail cooling rates has been extensively studied by embedding thermocouple experiments. Accelerated chilling of the rail profiles is also modeled in a lab to approximate its cyclic nature. The greatest significant influence on cooling speeds was determined to be the spray's strength (Zang, Zhang, Cui, and Gao, 2011).

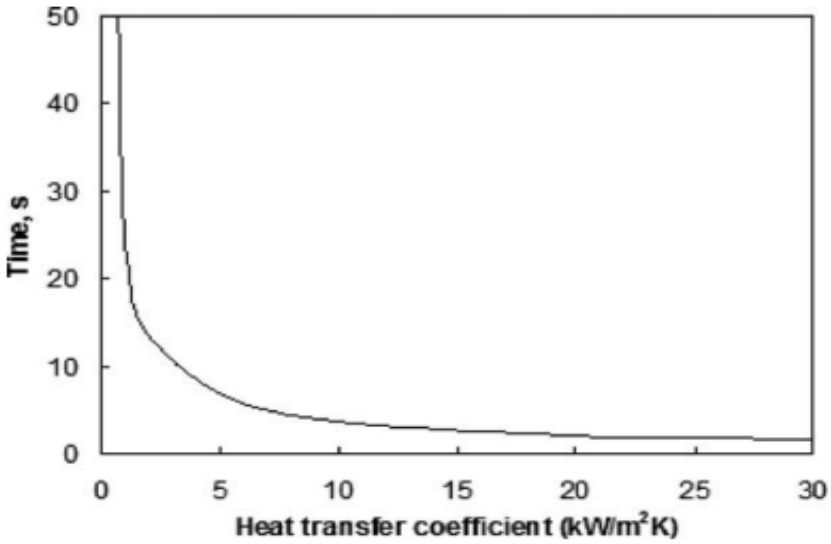

Figure.6: The period to reach 300°C at a point of 4 mm under the external steel platter from a twitch temperature of 500°C [source: (Su and Chwang, 2007)]

The ineffectiveness of increasing spray power when the cooling rate is limited by heat conduction first from the core toward the surface was demonstrated. There is evidence of this in Fig. 6.

2.3. Accelerated cooling:

The term "accelerated cooling" states to methods of precise preservation that are earlier than midair cooling, such as the use of an air-water fog, polymer, or aquatic cooling. At Brinkworth, a hot-strip mill in the United Kingdom, rapid cooling was first employed to reduce coiling temperature while improving mechanical properties without the need for a lengthy cooling zone after rolling (Polotskaya, 1988). As a result of accelerated cooling, new rail steel can be produced with reduced pearlite interlamellar spacing and poorer wear resistance because of the lower temperature required for phase transformation.

2.4. Microstructure and mechanical properties:

Austenite disperses into pearlite by nucleation and development. Carbon distribution did austenite limits this process. How this structure form affects its mechanical characteristics. Fine, 100% pearlitic assembly with short interlamellar space improves powered belongings, especially wear struggle. The lesser the interlayer space, the bigger the wear fighting, and depravity versa. Microstructures can change characteristics through transformation. Interlamellar spacing gets finer below the equilibrium transformation temperature and coarser above it.

3. Research methodology:

In this portion of the research, secondary data have been gathered from several sources, including books, articles in newspapers and journals, research reporters and published works, and websites.

3.1. Data acquisition:

This inquiry involved 900A rail steel. Fig. 7 displays railing steel's chemical composition. A light scanning electron microscope (LOM) was used to evaluate the microstructure, as shown in Fig. 8. The pearlitic structure was expected. The steel's median hardness was 258 HB after additional measurements. Comparing head and web rails' mechanical properties revealed no differences.

STEEL	C	Si	Mn	P	S	Cr	Ni
GRADE 900A	0.747	0.298	0.782	0.021	0.015	0.026	0.005

Figure.7: Biochemical configuration of the inspected toughen ranking 900A (in wt. %) [source: (Pittman, 2009)]

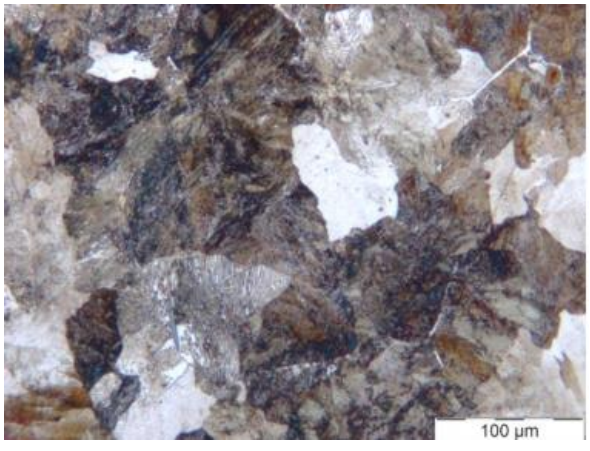

Figure.8: Detected microstructure of inspected rail steel [source: (Pittman, 2009)]

3.2. Data analysis:

Test tensile: Tensile tests determined the rail steel's mechanical characteristics. And lengthways the longitudinal way of the railing, ASTM E8 ductile specimens through a 6 mm gauge thickness and 24 mm gauge length were removed and manufactured (Fig. 9). Tensile tests were done at room temperature using 3 mm/min universal testing equipment. Digital image concordance (DIC) was used to measure deformed specimen elongations until breakage. Five tests were repeated.

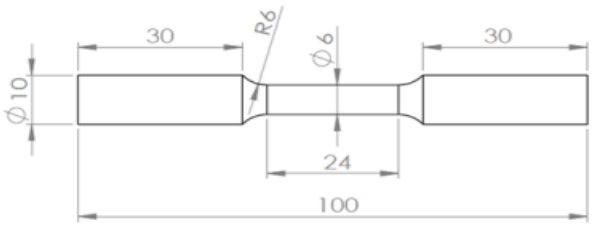

Figure.9: Geometry of stretchable example rendering to ASTM E8 average [source: (Pittman, 2009)]

Charpy testing: Fig. 9 shows the ASTM E23 Charpy test being used to determine rail steel toughness. The examples were pulled out and organized length wise along the track.

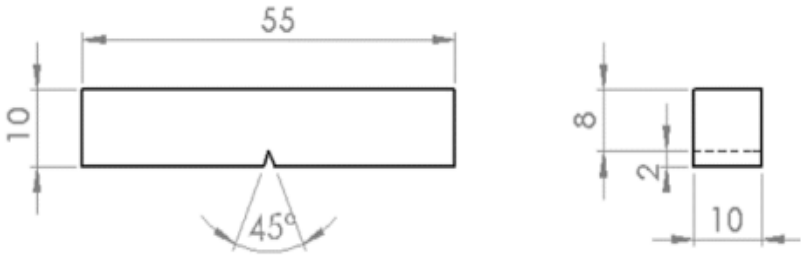

Figure.10: Geometry of charpy example rendering to ASTM E23 average [source: (Pittman, 2009)]

4. Result and discussion:

Fig. 10, shows the rail steel's stress-strain relationship. Grade 900A steel has modest elongation, yield, and tensile properties. Yield stress and workable strength remained 528 then 1029 MPa, individually. The strength values are near to pearlitic rail metal and meet UIC 860 requirements (Pittman, 2009). The Charpy test showed an impression of latent heat of 13.11 J, indicating minimal toughness.

RVE simulations were performed to produce the best plasticity stress-strain curve on rail steel with different phase fractions. Fig. 12a shows microstructures having 70% pearlite vs 30% bainite along with their stress-strain curves. Pearlite hardened faster than bainite at the start of

strain hardening. Bainite has higher flow stresses. Fig. 12 shows RVE model stress distributions (b). Bainite was stressed. Pearlite could sustain plastic strains, while calcite couldn't.

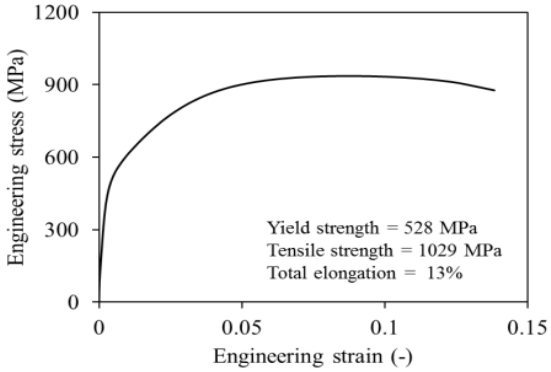

Figure.11: Empirically determined manufacturing stress-strain arc of the rail steel [source: (Pittman, 2009]

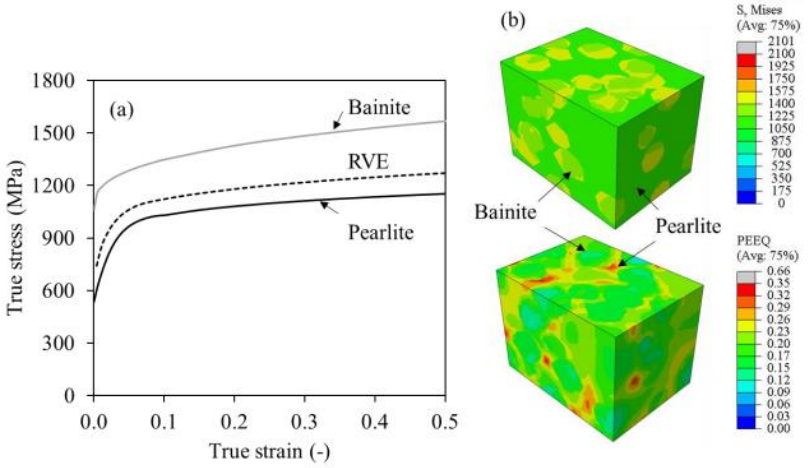

Figure.12: (a) Stress-strain arcs projected by RVE reproduction then (b) designed local pressure and strain disseminations for rail steel through 70% pearlite and 30% bainite microstructure [source: (Dong, Li, Somani and Misra, 2021)]

In microstructure flow stress arcs, crops besides stretchy characteristics matched bainitic phase fractions. Crossing stress and strain curves determined tensile strengths. With more bainite, yield and tensile strength increased. Equally (Dong, Li, Somani, and Misra, 2021). Figure 13 demonstrates ductility and pearls-bainitic microstructures. Figures 13(a) and 13(b) compare yield and tensile strengths. These findings will be tested.

5. Conclusion:

The grade 900A rail steel was examined for its microstructure and mechanical properties. With RVE simulations, the effects of bainite happening flow anxiety arcs, yielding besides tensile of different microstructure rail steel were then examined. Ultimate power and moderate flexibility, attended through a straining rate toughening rate there at the onset of ductile

materials, were evident in the pearlitic railroad steel grade 900A test specimens. As a result of an impact testing machine, the rail steel under investigation was found to have low toughness. Three-dimensional RVE models predicted the stress-strain answers for rail steel through varying amounts of bainite microstructure. Based on the data given here, we can infer connections between strength or bainitic phase fraction. The bainitic proportion had a greater impact on yield strength than the tensile strength, the researchers discovered.

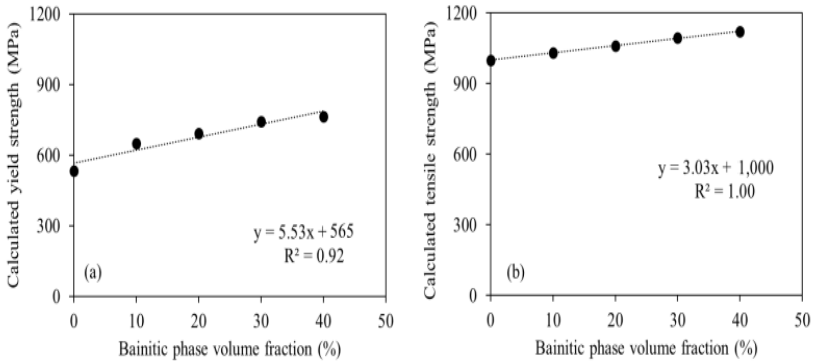

Figure.13: Foreseen relations among (a) yield strong point and (b) tensile asset and bainitic phase fraction of rail steel through pearlitic/bainitic microstructure [source: (Dong, Li, Somani and Misra, 2021)]

6. References:

1. Dean, s., kobasko, n., aronov, m., Powell, j. and totten, g., 2009. one more discussion "what is intensive quenching process?". journal of astm international, 6(1), p.101792.
2. Dong, h., li, z., somani, m. and misra, r., 2021. The significance of phase reversion-induced nanograined/ultrafine-grained (ng/ufg) structure on the strain hardening behavior and deformation mechanism in copper-bearing antimicrobial austenitic stainless steel. Journal of the mechanical behaviour of biomedical materials, 119, p.104489.
3. Eustis, j., 2013. Tech services on the web: steven j. miller's metadata resources page https://pantherfile.uwm.edu/mll/www/resource.html. Technical services quarterly, 30(2), pp.237-238.
4. Georgiev, m. and simeonova, t., 2019. crack resistance of volume-hardened railroad rails with transverse cracks in the head. Metal science and heat treatment, 60(11-12), pp.814-816.
5. Grushko, s., vysocky, a., suder, j., glogar, l. and bobovsky, z., 2021. improving human awareness during collaboration with robot: review. mm science journal, 2021(6), pp.5475-5480.
6. Hall, d. and mudawar, i., 1996. Optimization of quench history of aluminum parts for superior mechanical properties. international journal of heat and mass transfer, 39(1), pp.81-95.
7. Kazum, o., kannan, m., beladi, h., timokhina, i., hodgson, p. and khoddam, s., 2013. selective dissolution of retained austenite in nanostructured bainitic steels. Advanced engineering materials, 16(4), pp.442-444.

8. Khukharev, a., 1974. Methods used by steelmaker v. i. danilenko. Metallurgist, 18(1), pp.43-44.
9. Krauss, g., 1995. Heat treated martensitic steels: microstructural systems for advanced manufacture. isij international, 35(4), pp.349-359.
10. Long, x. and khanna, s., 2007. fatigue properties and failure characterization of spot welded high strength steel sheet. international journal of fatigue, 29(5), pp.879-886.
11. Luo, x. and totten, g., 2014. distortion control: quenching apparatus for hardening parts: an overview. materials performance and characterization, 3(4), p.20130086.
12. Masoudi nejad, r. and liu, z., 2021. analysis of fatigue crack growth under mixed-mode loading conditions for a pearlitic grade 900a steel used in railway applications. engineering fracture mechanics, 247, p.107672.
13. Olofsson, u., zhu, y., abbasi, s., lewis, r. and lewis, s., 2013. tribology of the wheel–rail contact – aspects of wear, particle emission and adhesion. vehicle system dynamics, 51(7), pp.1091-1120.
14. Pittman, m., 2009. first aid manual – ninth edition first aid manual – ninth edition. nursing standard, 23(37), pp.30-30.
15. Polotskaya, r., 1988. thermodynamic properties of higher lanthanum silicide. soviet powder metallurgy and metal ceramics, 27(2), pp.154-155.
16. Su, j. and chwang, a., 2007. estimation of heat transfer coefficient of cryogen spray cooling with alifanov's iterative regularization method. numerical heat transfer, part a: applications, 51(8), pp.781-794.
17. Toribio, j., gonzález, b. and matos, j., 2013. strength anisotropy and mixed mode fracture in heavily drawn pearlitic steel. fatigue & fracture of engineering materials & structures, 36(11), pp.1178-1186.
18. Zang, y., zhang, b., cui, l. and gao, z., 2011. The analysis of temperature field and residual stress distribution during h-beam cooling process. Advanced materials research, 194-196.

Cite as

Sonali Shinde[1], Parishwad Gaeakwad*[2]. Shibanjan Paul Roy[3] (2023). Study of Mechanical Properties of Pearlitic Rail Steel by Modeling.
https://doi.org/10.5281/zenodo.8054087